Submitted to the
XXXIst International Conference on High Energy Physics
24–31 July 2002, Amsterdam, The Netherlands

Abstract: 813 **Parallel Session(s): 6,5**

Exclusive electroproduction of J/ψ mesons at HERA

ZEUS Collaboration

Abstract

Exclusive electroproduction of J/ψ mesons in ep collisions, $ep \to eJ/\psi p$, has been studied with the ZEUS detector at HERA using an integrated luminosity of 82 pb^{-1}. The cross section is measured for γp center-of-mass energies $30 < W < 220$ GeV in two ranges of the four-momentum transfer at the lepton vertex, $0.15 < Q^2 < 0.8$ GeV^2 and $Q^2 > 2$ GeV^2. Cross sections are shown as a function of Q^2, W and t, the four-momentum-transfer squared at the proton vertex. The ratio of the cross sections, $\sigma(J/\psi)/\sigma(\rho)$, is presented as a function of Q^2. The t-dependence of the J/ψ cross sections is measured for $Q^2 > 2$ GeV^2.

1 Introduction

Elastic photoproduction of light vector mesons (VMs) (ρ, ω and ϕ) has been measured both in fixed-target experiments [1] and at HERA [2–4]. At sufficiently high photon-proton centre-of-mass energies ($W > 10\,\mathrm{GeV}$), the reactions display the characteristics of soft diffractive processes, most notably a slow rise of the cross section ($\propto W^{\delta}$, $\delta \simeq 0.22$). This behaviour is well described by the vector dominance model (VDM) [5] in conjunction with Regge phenomenology [6].

A different behaviour has been observed for the J/ψ photoproduction cross section [7,8], which rises more rapidly with W ($\delta \simeq 0.6 - 0.9$). This observation is inconsistent with a soft production mechanism. An alternative approach based on perturbative QCD (pQCD) has been proposed for VM production in the presence of a hard scale [9,10]. The reaction is understood as a scattering, mediated by two gluons in a colour-singlet state, between the proton and a colour dipole ($q\bar{q}$) into which the photon fluctuates. The cross section is approximately proportional to the square of the gluon density in the proton, $[xg(x,\mu^2)]^2$, where the hard scale μ^2 is given by $M_{J/\psi}$. The observed steep rise in the cross section is explained by the rapid increase of the gluon density towards low x, since $W^2 \propto 1/x$.

A similar behaviour is observed in the exclusive electroproduction of light vector mesons, where the hard scale may be provided by a combination of M_V^2 and Q^2, the negative four-momentum squared of the virtual photon. The observed W dependence [11, 12] at Q^2 values close to the J/ψ-mass squared ($Q^2 \approx M_{J/\psi}^2$) yield values of δ ($\simeq 0.4 - 0.7$), similar to those obtained for photoproduction of J/ψ . It is therefore interesting to study the cross-section behaviour of elastic J/ψ production in the presence of two scales, Q^2 and $M_{J/\psi}^2$, at various values of Q^2.

The results in this paper are based on $82\,\mathrm{pb}^{-1}$ of ZEUS data taken in 1998-2000, when HERA ran with a 920 GeV proton beam and a 27.5 GeV electron or positron beam. The cross section $\sigma_{\gamma^* p \to J/\psi p}$ is presented as a function of Q^2, at $W = 90\,\mathrm{GeV}$, for the two Q^2 ranges $0.15 < Q^2 < 0.8\,\mathrm{GeV}^2$ and $Q^2 > 2\,\mathrm{GeV}^2$. The Q^2 dependence is compared with that of ρ electroproduction, $\sigma_{\gamma^* p \to \rho p}$, by taking the ratio $\sigma_{J/\psi}/\sigma_{\rho}$ as a function of Q^2 .

The cross sections are also presented as a function of W for both Q^2 ranges. The analysis for $Q^2 > 2\,\mathrm{GeV}^2$ has an extended W range $30 < W < 220\,\mathrm{GeV}$ compared to $50 < W < 150\,\mathrm{GeV}$ in an earlier study [13]. In addition, the differential cross-section $d\sigma_{\gamma^* p \to J/\psi p}/dt$, where t is the squared four-momentum-transfer at the proton vertex, is measured for $Q^2 > 2\,\mathrm{GeV}^2$.

2 Kinematics

The following kinematic variables are used for describing exclusive VM production: k, k', P, P' and q, the four-momenta of the incident lepton, scattered lepton, incident proton, scattered proton and virtual photon, respectively; $Q^2 = -q^2 = -(k - k')^2$, the negative four-momentum squared of the virtual photon; $W^2 = (q + P)^2$, the squared invariant mass of the photon-proton system; $y = (P \cdot q)/(P \cdot k)$, the fraction of the positron[1] energy transferred to the photon in the proton rest frame; and $t = (P - P')^2$, the squared four-momentum-transfer at the proton vertex.

The kinematic variables were reconstructed using the "constrained" method [11]. The two leptonic decay channels, $J/\psi \to e^+e^-$ and $J/\psi \to \mu^+\mu^-$ were used for the high-Q^2 data. Only e^+e^- decays were used for the low-Q^2 analysis. The momenta of the muons were measured by the central tracking detector (CTD) [14]. In the case of e^+e^- decays, the events with one electron candidate in the CTD and another electromagnetic cluster in the uranium calorimeter [15] outside the angular coverage of the CTD were also used (one-track events). This allows an extention of the W range from the previous measurement of $50 < W < 150\,\text{GeV}$ to $30 < W < 220\,\text{GeV}$. The sample was added to that containing two charged tracks in the CTD (two-track events).

3 Results

3.1 Data characteristics

Figure 1 shows the distribution of the dilepton invariant mass, M_{ll}, for various samples of J/ψ events. The corresponding mass spectrum for dielectron events for $0.15 < Q^2 < 0.8\,\text{GeV}^2$ is shown in Figure 2.

The mass spectra in Fig. 1 are compared with the sum of the J/ψ signal simulated by the ZEUSVM [16] Monte Carlo generator interfaced to HERACLES 4.6.1 [17] and the non-resonant QED production of e^+e^-- and $\mu^+\mu^-$-pairs, simulated by the GRAPE-Dilepton 1.1 [18] generator. For $0.15 < Q^2 < 0.8\,\text{GeV}^2$, the LPAIR [18] generator is used for the estimation of the non-resonant QED background. The ZEUSVM prediction was normalised to the sum of the number of events observed in the mass range $2.6 < M_{ee} < 3.4\,\text{GeV}$ and $2.8 < M_{\mu\mu} < 3.4\,\text{GeV}$ for the electron and muon decay channels, respectively, after the subtraction of the non-resonant background. The mass spectra are well described by the combination of these Monte Carlo programs.

[1] Here "positron" represents the incoming lepton-beam particle type, either electron or positron.

3.2 Cross sections

The cross sections were corrected to the entire $|t|$ range, assuming an exponential behaviour of the cross section in t, as measured and presented in Section 3.4.

The total cross section, $\sigma^{\gamma^* p \to J/\psi p}$, is presented as a function of W and Q^2. The W dependence is shown in Fig. 3 for four Q^2 ranges: $0.15 < Q^2 < 0.8\,\mathrm{GeV}^2$; $2 < Q^2 < 5\,\mathrm{GeV}^2$; $5 < Q^2 < 10\,\mathrm{GeV}^2$; and $10 < Q^2 < 100\,\mathrm{GeV}^2$. Also shown is the photoproduced J/ψ cross sections measured by H1 [8] and ZEUS [7]. A strong rise in W is observed for all regions of Q^2.

The cross sections are also compared with theoretical predictions from Martin et al. (MRT) [19] using CTEQ5M [20], and from Frankfurt et al. (FKS) [21] using CTEQ4M [22]. Since the prediction from FKS underestimates the magnitude of the measured cross section, it was multiplied by 1.66. The magnitude of the MRT prediction was not modified. The W dependence of the cross section predicted by MRT reproduces the data well. The dependence in the FKS model tends to be steeper than the data.

The cross sections for each Q^2 bin have been fitted with the functional form W^δ. The result is $\delta = 0.84 \pm 0.38(stat.)^{+0.10}_{-0.04}(syst.)$, $0.72 \pm 0.18^{+0.17}_{-0.07}$, $0.64 \pm 0.18^{+0.12}_{-0.14}$ and $1.10 \pm 0.15^{+0.15}_{-0.15}$ for $Q^2 = 0.4, 3.1, 6.8$ and $16\,\mathrm{GeV}^2$. These δ values are shown as a function of Q^2 in Fig. 4. They can be compared with the values measured for photoproduction: $0.83 \pm 0.07(stat. \oplus syst.)$ by H1 [8] and $0.69 \pm 0.02(stat.) \pm 0.03(syst.)$ by ZEUS. No strong dependence of δ on Q^2 is observed.

The Q^2 dependence, measured at $W = 90\,\mathrm{GeV}$ by integrating over the ranges $30 < W < 220\,\mathrm{GeV}$ for $0.1 < Q^2 < 0.9$ and $46 < W < 140\,\mathrm{GeV}$ for $Q^2 > 2\,\mathrm{GeV}^2$, are presented in Fig. 5. Also shown are the photoproduction measurements by H1 [8] and the value from ZEUS [7] interpolated to $W = 90\,\mathrm{GeV}$. The cross sections for all the Q^2 range, from $Q^2 = 0$ to $100\,\mathrm{GeV}^2$, were fitted with the parameterisation $1/(Q^2 + M^2_{J/\psi})^n$, yielding $n = 2.70 \pm 0.08(stat.)$ with $\chi^2/\mathrm{dof} = 2.02$. Such a function, shown in Fig. 5, does not give a good description of the ZEUS data for $Q^2 > 5\,\mathrm{GeV}^2$. The Q^2 dependence is also compared with the predictions of MRT with CTEQ5M and of FKS using CTEQ4M. The prediction from MRT with CTEQ5M gives a good description of the measured cross section both in magnitude and shape. The normalized FKS gives a fairly good description of the Q^2 dependence of the data.

3.3 Cross section ratio $\sigma_{J/\psi}/\sigma_\rho$

In VDM, the ratios of the different VM cross sections are given by the coupling of the photon to the VMs and by the elastic VM-proton cross sections. Under the simple assumption that the photon-VM coupling is proportional to the quark-current decomposition of the photon (SU(4) flavour symmetry), and that the VM-proton cross sections are universal, the cross-section ratio is given by $\rho : \omega : \phi : J/\psi = 9 : 1 : 2 : 8$. For the cross section ratio at a given Q^2, this prediction is expected to hold in the region where the mass of the vector meson can be ignored, i.e. $Q^2 \gg M_V^2$.

In the pQCD approach, the coupling strength between the exchanged two-gluon system and the dipole is assumed to be universal. However, the coupling between the dipole and the VM wave-function is expected to be proportional to the mass of the VM. Therefore the ratio becomes larger for heavy VMs: $\rho : \omega : \phi : J/\psi = 9 : 0.8 : 2.4 : 28$ [10].

The ratio, $r = \sigma^{\gamma^* p \to J/\psi p}/\sigma^{\gamma^* p \to \rho p}$ is shown as a function of Q^2 at $W = 90\,\text{GeV}$ in Fig. 6. The extraction of the ρ cross section is discussed elsewhere [23]. Figure 6 also shows the measurements from H1 [24] and the previous ZEUS measurements in photoproduction [25] and electroproduction [11]. The ratio rises rapidly as Q^2 increases. However, it is below 8/9 even at the highest Q^2 and is much lower than the value of 28/9 expected from pQCD.

3.4 The differential cross section $d\sigma_{\gamma^* p \to J/\psi p}/dt$

The t-dependence of the cross section can be parametrised as $d\sigma/dt \propto e^{-bt}$, where b represents the size of the interaction. The small value of this parameter, $b \simeq 4.5\,\text{GeV}^{-2}$, observed for J/ψ photoproduction [7, 8] as well as for high-Q^2 ρ production [11, 12], is comparable to the size of the proton, implying a much smaller size for the virtual photon. Therefore, these observations can be considered as evidence of a point-like interaction mechanism in vector-meson production when a hard scale is present.

Figure 7 shows the differential cross-section $d\sigma_{\gamma^* p \to J/\psi p}/dt$ for $Q^2 > 2\,\text{GeV}^2$. The cross section is well described by an exponential function e^{bt}, with a fitted value of $b = 4.63 \pm 0.20(stat.)^{+0.32}_{-0.36}(syst.)\,\text{GeV}^{-2}$. The cross section is also fitted using an elastic form factor for the two-gluon exchange, $(1 - t/m_{2g}^2)^{-4}$ [26], yielding $m_{2g}^2 = 0.57\,\text{GeV}^2$. This also describes the data well.

The b parameter is measured in three ranges of Q^2. These are compared to other measurements of the J/ψ production at high Q^2 [24] and the photoproduction measurements [7, 8], as shown in Fig. 8. No evidence of a variation in Q^2 is found; an average value $\langle b \rangle = 4.5 \pm 0.2\,\text{GeV}^{-2}$ is consistent with all the measurements.

Acknowledgment

We thank the DESY directorate for their strong support and encouragement, and the HERA machine group for their diligent efforts. It is also a pleasure to thank Leonid

Frankfurt, Werner Koepf, Mark Strikman and Thomas Teubner for providing us with their model predictions and for fruitful discussions.

References

[1] R.M. Egloff et al., Phys. Rev. Lett. **43**, 657 (1979);
R.M. Egloff et al., Phys. Rev. Lett. **43**, 1545 (1979);
D. Aston et al., Nucl. Phys. **B 209**, 56 (1982);
J. Busenitz et al., Phys. Rev. **D 40**, 1 (1989);
For a review of earlier results, see T.H. Bauer et al., Rev. Mod Phys. **50**, 261 (1978); Erratum ibid. **51**, 407 (1979); and references therein.

[2] ZEUS Coll., M. Derrick et al., Z. Phys. **C 69**, 39 (1995);
H1 Coll., S. Aid et al., Nucl. Phys. **B 463**, 3 (1996).

[3] ZEUS Coll., J. Breitweg et al., Eur. Phys. J. **C 2**, 247 (1998);
ZEUS Coll., M. Derrick et al., Z. Phys. **C 73**, 73 (1996).

[4] ZEUS Coll., M. Derrick et al., Phys. Lett. **B 377**, 259 (1996).

[5] J.J. Sakurai, Ann. Phys. **11**, 1 (1960).

[6] P.D.B. Collins, *An Introduction to Regge Theory and High Energy Physics.* Cambridge University Press (1977).

[7] ZEUS Coll., S. Chekanov et al., Preprint DESY-02-008, hep-ex-0201043, DESY, 2002. Subm. to Eur. Phys. J.

[8] H1 Coll., C. Adloff et al., Phys. Lett. **B 483**, 23 (2000).

[9] S.J. Brodsky et al., Phys. Rev. **D 50**, 3134 (1994).

[10] L. Frankfurt, W. Koepf and M. Strikman, Phys. Rev. **D 54**, 3194 (1996).

[11] ZEUS Coll., J. Breitweg et al., Eur. Phys. J. **C 6**, 603 (1999).

[12] H1 Coll., C. Adloff et al., Eur. Phys. J. **C 13**, 371 (2000).

[13] ZEUS Coll., Abstract 879, XXXth International Conference on High Energy Physics ICHEP2000, Osaka, Japan, 2000, available on `http://www-zeus.desy.de/physics/phch/conf/osaka_paper/DIFF/jpsidis.ps.gz`.

[14] N. Harnew et al., Nucl. Inst. Meth. **A 279**, 290 (1989);
B. Foster et al., Nucl. Phys. Proc. Suppl. **B 32**, 181 (1993);
B. Foster et al., Nucl. Inst. Meth. **A 338**, 254 (1994).

[15] M. Derrick et al., Nucl. Inst. Meth. **A 309**, 77 (1991);
A. Andresen et al., Nucl. Inst. Meth. **A 309**, 101 (1991);
A. Caldwell et al., Nucl. Inst. Meth. **A 321**, 356 (1992);
A. Bernstein et al., Nucl. Inst. Meth. **A 336**, 23 (1993).

[16] K. Muchorowski, Ph.D. Thesis, Warsaw University, Warsaw, Poland (1996) (unpublished).

[17] A. Kwiatkowski, H. Spiesberger and H.-J. Möhring, Comp. Phys. Comm. **69**, 155 (1992). Also in *Proc. Workshop Physics at HERA*, 1991, DESY, Hamburg.

[18] T. Abe, Comp. Phys. Comm. **136**, 126 (2001).

[19] A.D. Martin, M.G. Ryskin and T. Teubner, Phys. Rev. **D 62**, 14022 (2000).

[20] CTEQ Coll., H.L. Lai et al., Eur. Phys. J. **C 12**, 375 (2000).

[21] L. Frankfurt, W. Koepf and M. Strikman, Phys. Rev. **D 57**, 512 (1998).

[22] H.L. Lai et al., Phys. Rev. **D 55**, 1280 (1997).

[23] ZEUS Coll., Abstract 880, XXXth International Conference on High Energy Physics ICHEP2000, Osaka, Japan, 2000, available on `http://www-zeus.desy.de/physics/phch/conf/osaka_paper/DIFF/rhodis.ps.gz`.

[24] H1 Coll., C. Adloff et al., Eur. Phys. J. **C 10**, 373 (1999).

[25] ZEUS Coll., J. Breitweg et al., Z. Phys. **C 75**, 215 (1997).

[26] L. Frankfurt and M. Strikman, Preprint hep-ph/0205223.

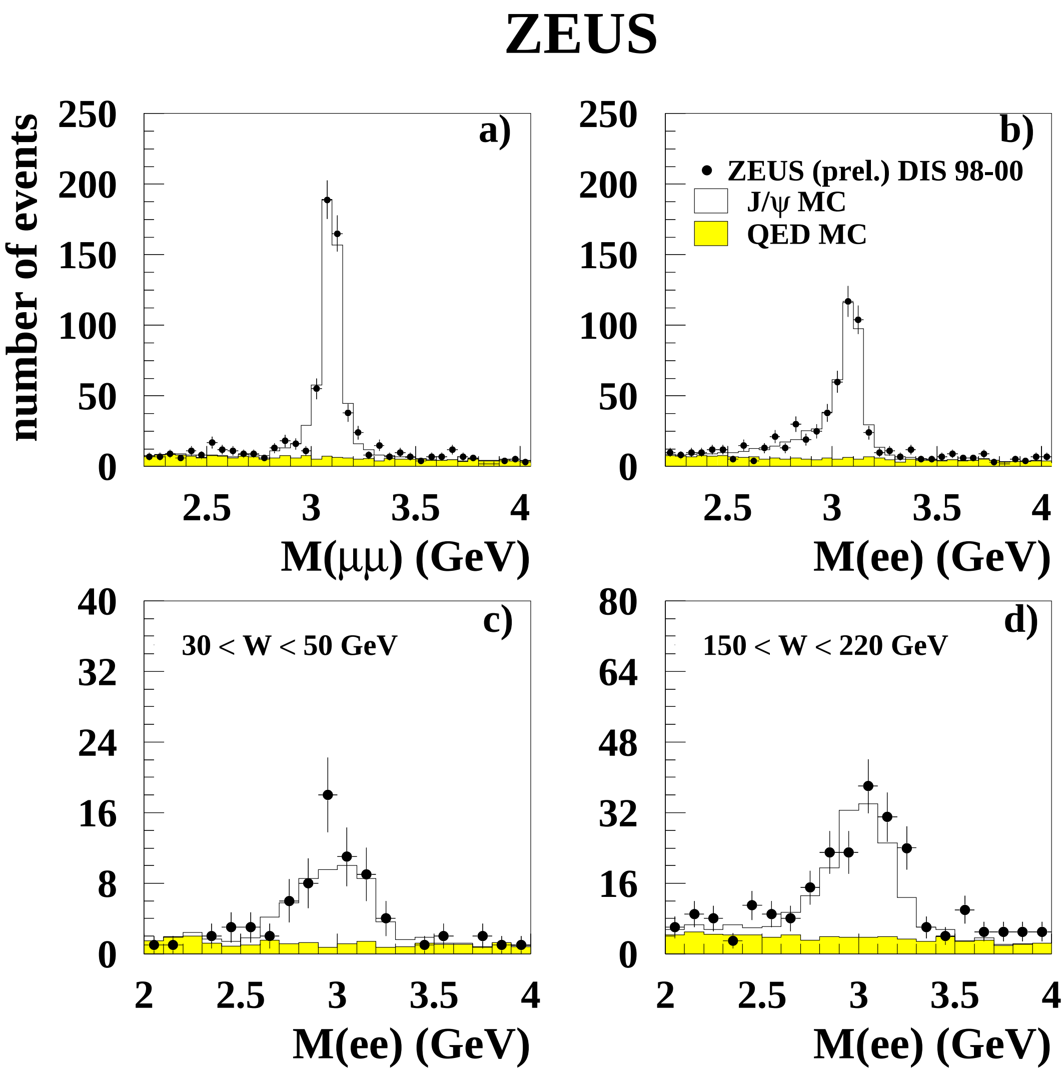

Figure 1: *The invariant mass distributions for* $Q^2 > 2\,GeV^2$*: a)* $\mu^+\mu^-$ *pairs and b)* e^+e^- *pairs from the two-track sample, c) the low-*W *one-track and d) the high-*W *one-track samples. The data are not corrected for detector acceptance effects. The solid histogram shows the sum of the ZEUSVM (*J/ψ *production) and GRAPE (QED non-resonant processes) Monte Carlo simulations, while the shaded histogram shows the contribution from GRAPE alone. The magnitude of the cross section from GRAPE is taken from the generator.*

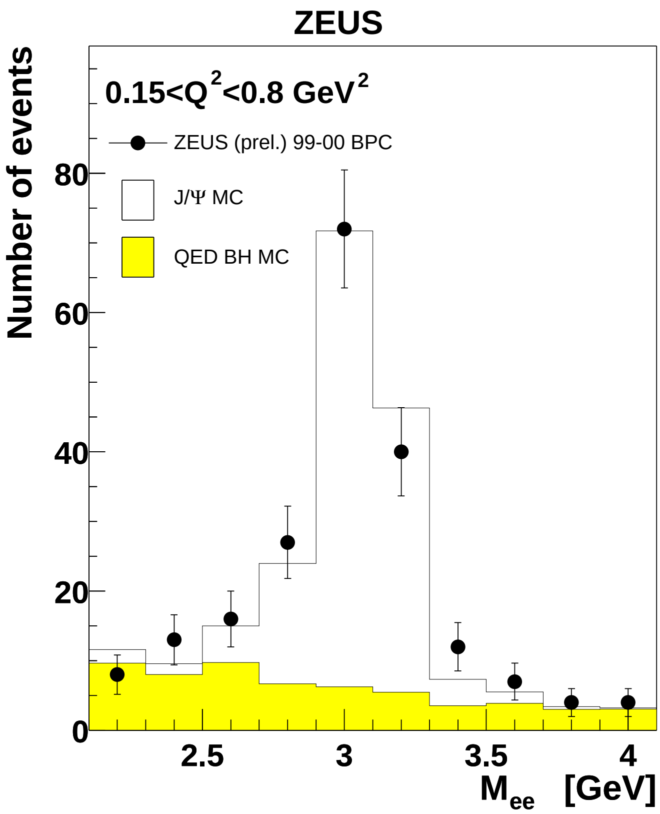

Figure 2: *The invariant mass distribution in the range* $0.15 < Q^2 < 0.8\,GeV^2$ *and* $30 < W < 220\,GeV$ *for* e^+e^- *pairs from both one- and two-track samples.*

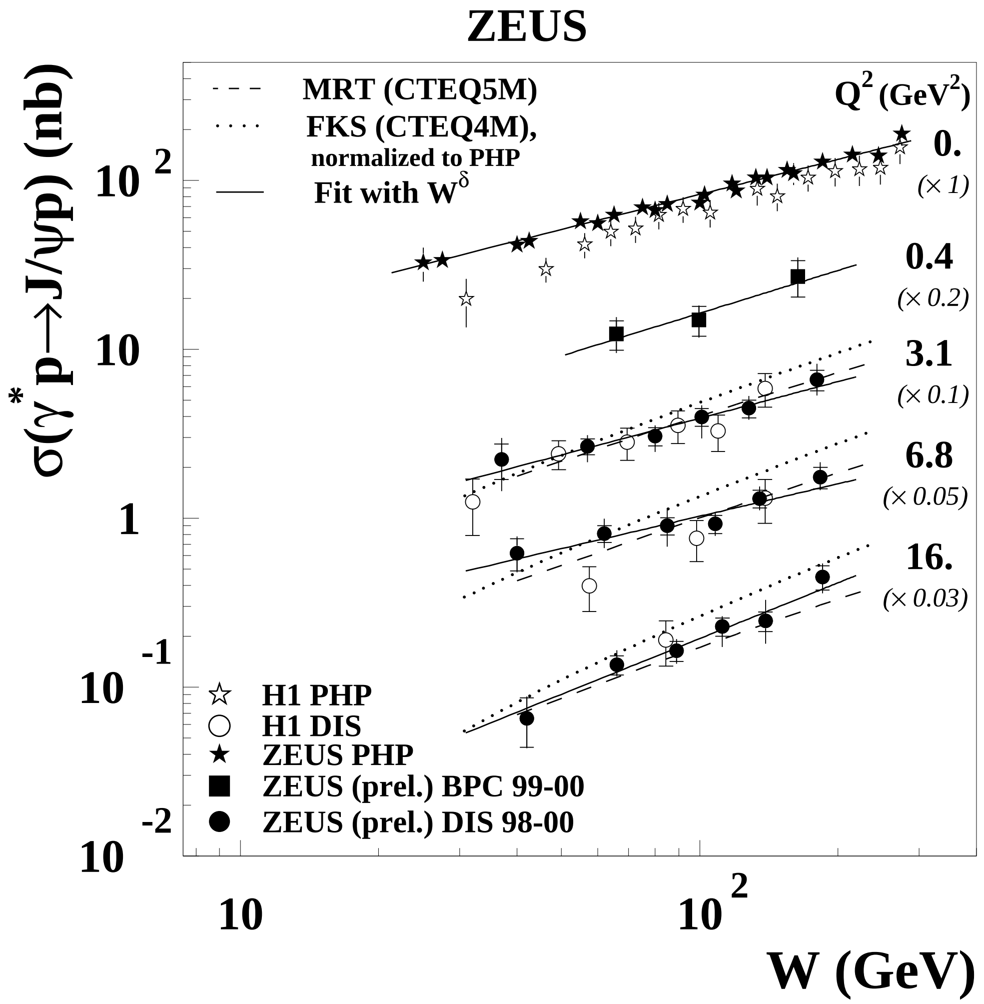

Figure 3: *The J/ψ cross section, $\sigma^{\gamma^* p \to J/\psi p}$, measured as a function of W for several ranges of Q^2. Each Q^2 range is multiplied by the constant shown in parenthesis for ease of display. The solid line indicates the result of a fit to the form W^δ for each Q^2 region. The dotted and dashed curves are the theoretical predictions from Frankfurt, Koepf and Strikman and Martin, Ryskin and Teubner, respectively.*

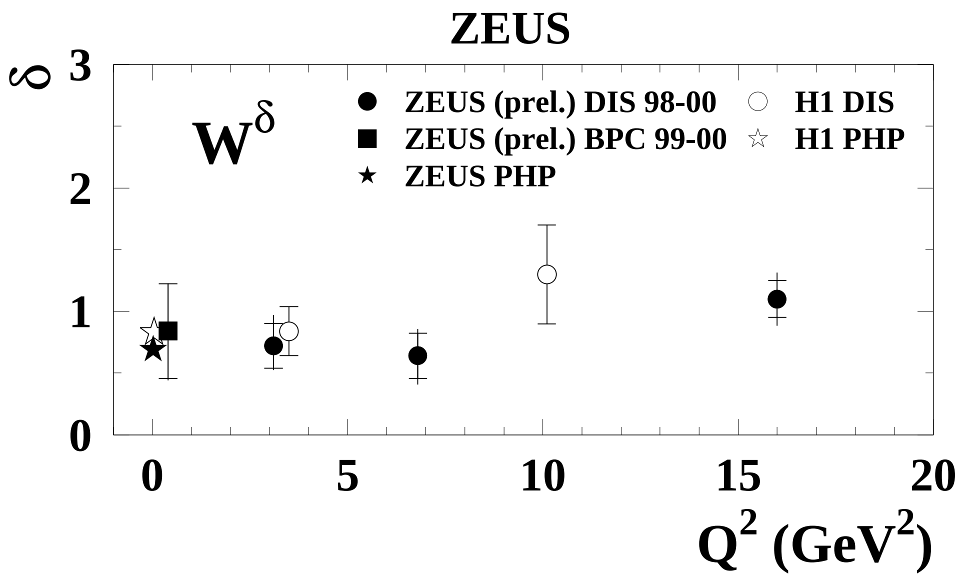

Figure 4: *The values of δ as a function of Q^2 for the fit to the data in Figure 3.*

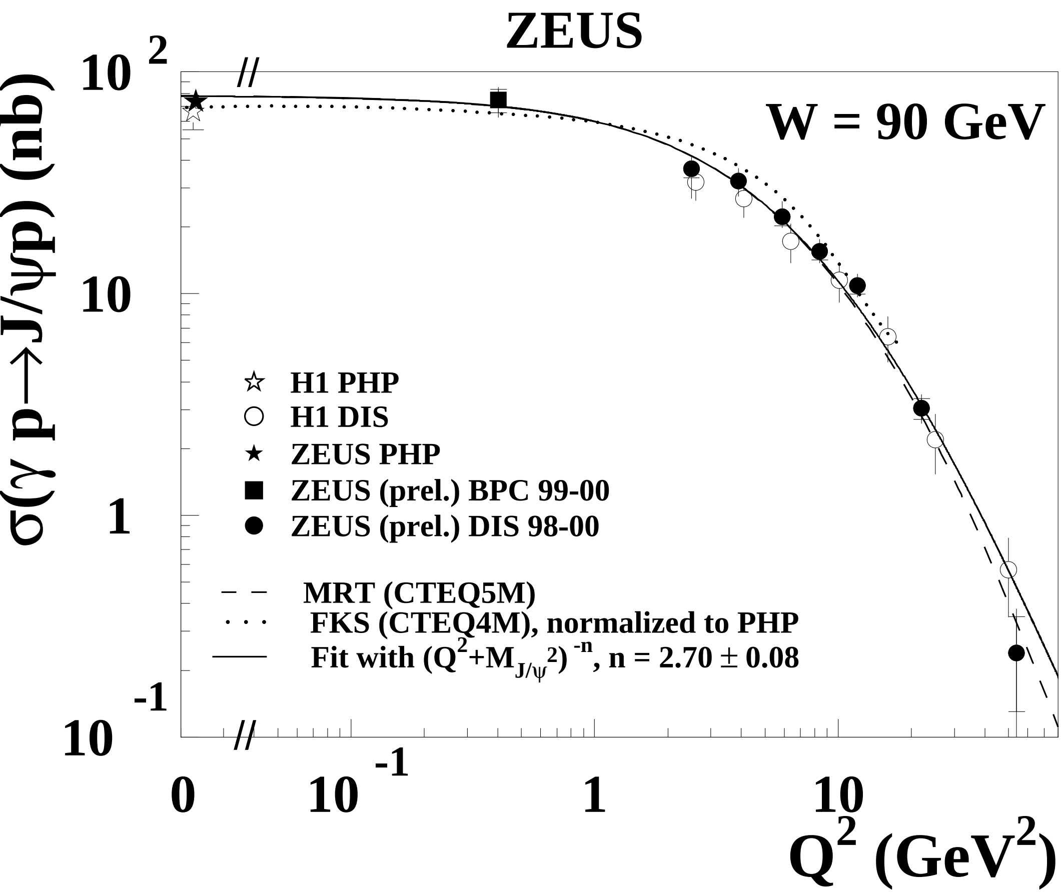

Figure 5: *The cross-section $\sigma^{\gamma^* p \to J/\psi p}$ as a function of Q^2, measured at $W = 90\,GeV$. The solid curve shows a fit to the function $\sigma_{\rm tot}^{\gamma^* p} \propto (Q^2 + M_{J/\psi}^2)^{-n}$ for all the ZEUS data shown. The dashed and dotted curves represent the theoretical predictions from FKS and MRT, respectively. The prediction for MRT in the Q^2 range below 5 GeV overlaps with the solid curve.*

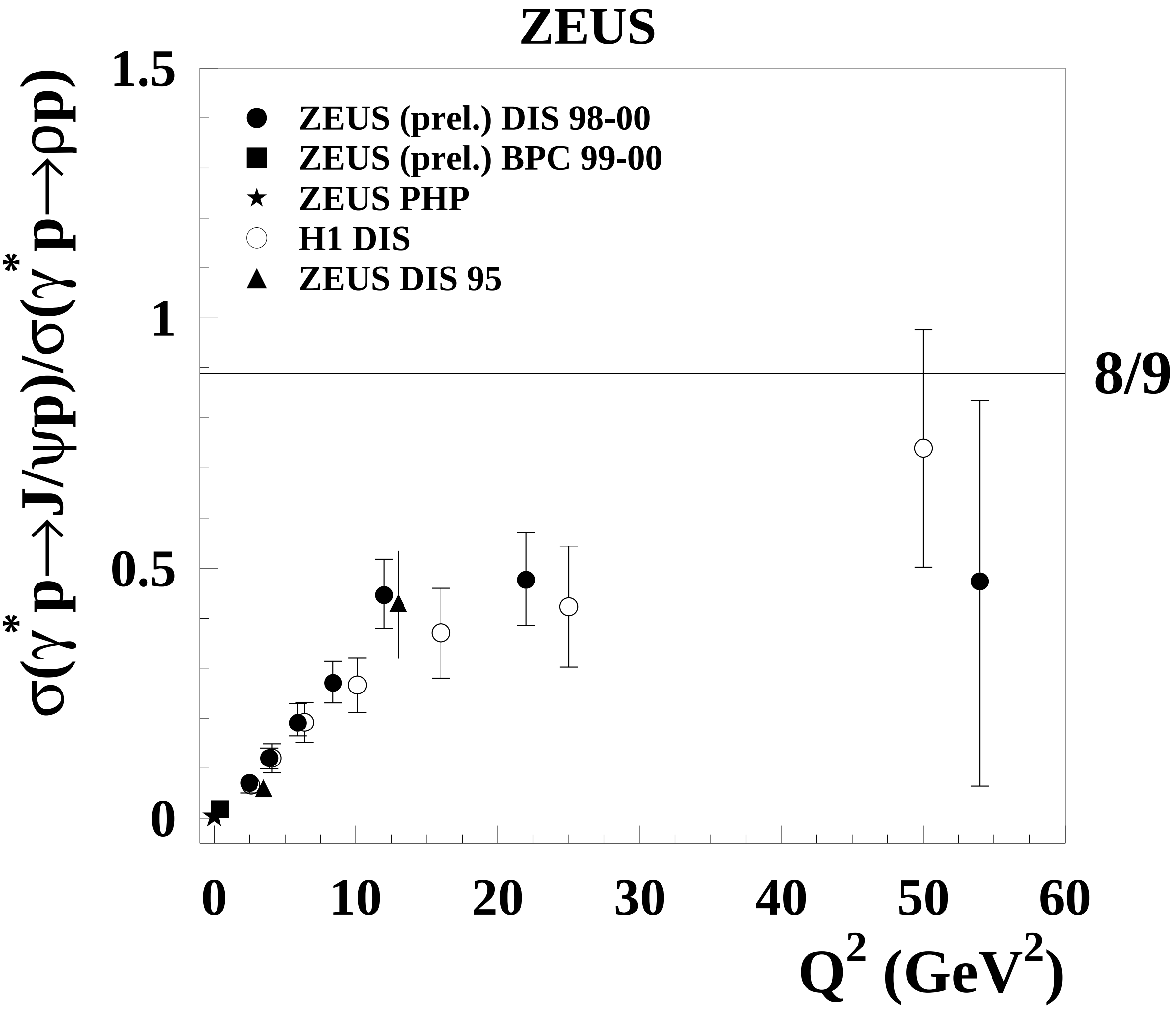

Figure 6: *The ratio of cross-sections $\sigma_{\mathrm{tot}}^{\gamma^* p \to \rho p}/\sigma_{\mathrm{tot}}^{\gamma^* p \to \rho p}$ as a function of Q^2. The uncertainty is given by the statistical error on the ρ and J/ψ cross sections and the systematic uncertainty on the J/ψ cross sections added in quadrature. The ρ cross sections were interpolated to the (W, Q^2) point of the J/ψ measurement.*

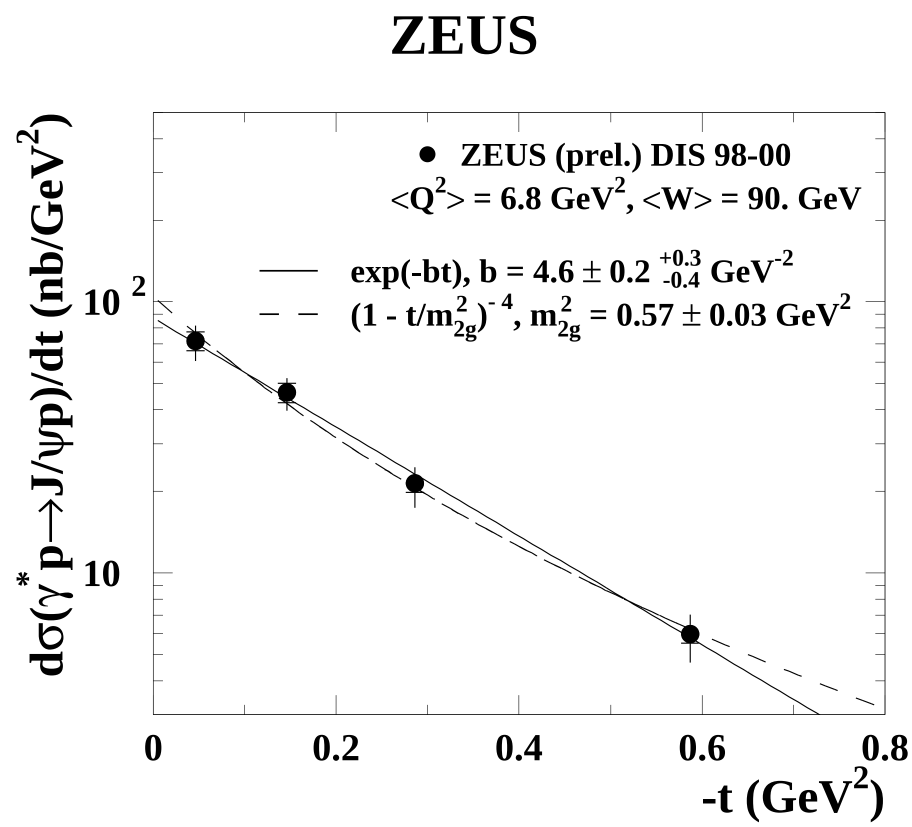

Figure 7: *The differential cross-section $d\sigma(\gamma^* p \to J/\psi p)/dt$. The solid line shows a fit to the function $d\sigma/dt \propto e^{bt}$. The dashed curve is a fit to the function $(1 - t/m_{2g}^2)^{-4}$, which represents the elastic form factor of the two-gluon exchange of the nucleon with the parameter m_{2g} obtained from the fit to the data.*

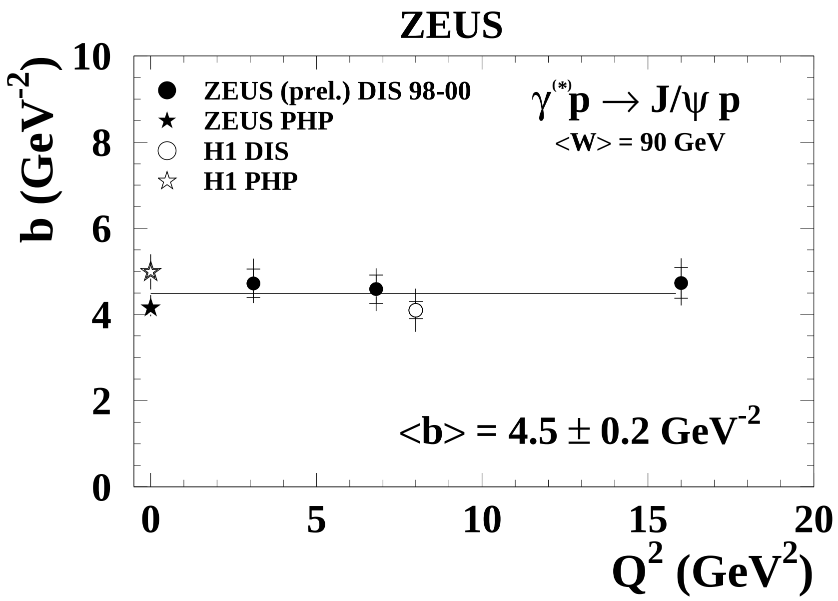

Figure 8: *The values of the b-slope parameter, $d\sigma/dt \propto e^{bt}$, as a function of Q^2. The horizontal line shows the avarage of all the points weighted by their statistical significance, giving $b = 4.5 \pm 0.2\ GeV^{-2}$.*